geoconvention Virtual Event September 13 - 15 2021

Field testing of multicomponent DAS sensing

Kevin W. Hall[1], Kristopher A.H. Innanen[1] and Donald C. Lawton[1,2]
[1]CREWES, University of Calgary, [2]Containment and Monitoring Institute

Summary

An experimental Directional DAS Sensor (DDS) was buried at the Containment and Monitoring Institutes Field Research Station (CaMI.FRS) in 2018 (Innanen et al., 2019; Hall et al., 2020). The sensor consists of two 10x10 m horizontal square loops of fibre buried at 2 m depth, with the second square rotated forty-five degrees relative to the first. A fibre loop was constructed consisting of: (1) straight fiber travelling clockwise around square one twice, (2) straight fibre clockwise around square 2 twice, (3) helically wound fibre clockwise around square 1 twice, and (4) helically wound fibre clockwise around square 1 twice. Three-component geophones were planted in undisturbed ground on the surface just outside of the corners of the DDS, oriented to magnetic North. We recorded four Vibe Points (VP) on the DDS in 2018 at four different offsets and two different azimuths. This abstract presents a method to estimate time series of strain-rate tensors from the straight and helical fiber data, as well as from horizontal components of the surface geophone data and shows a comparison of those results. Due to data constraints, primarily small source-receiver offsets, the method was attempted on the first peak of the first ground-roll arrival and gave us results consistent with what we would expect given the survey geometry.

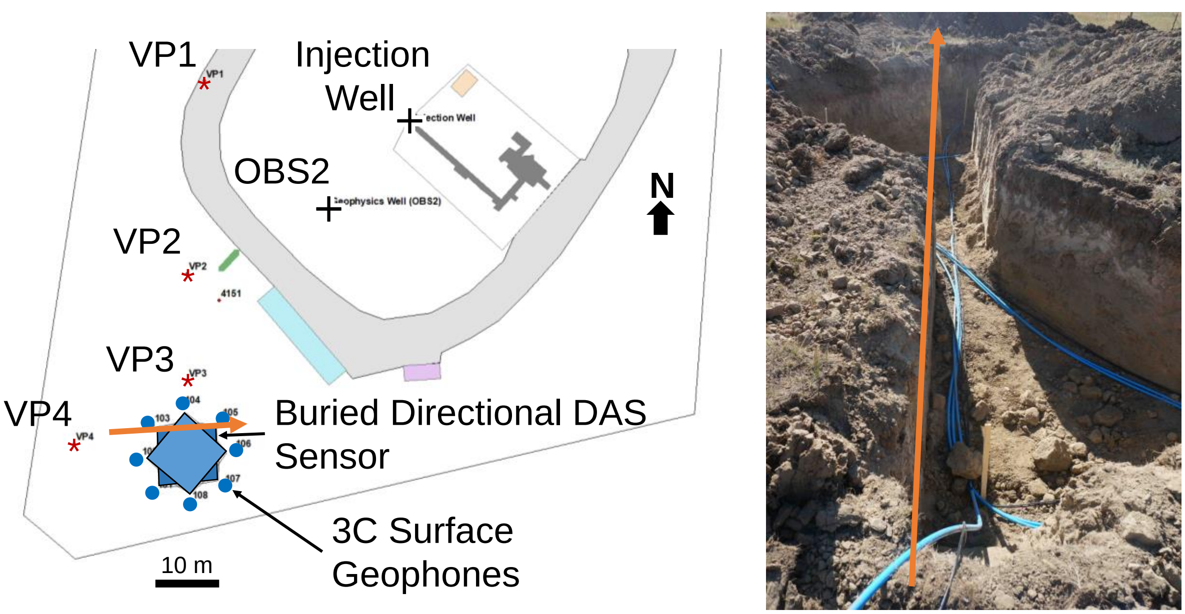

Figure 1. (Right) Directional DAS sensor (blue square), surface geophones (blue dots) and vibe point locations (red asterisks). (Left) Photo of the straight fibre cable (black) and helical fibre cable (blue), where the orange arrow on the map and the photographs are pointing in the same direction.

Method

If it were possible to construct a true "multicomponent" sensor, it would generate 6 independent traces. At each sample point, the 6 numbers would represent the instantaneous values of the 6 independent components of strain-rate that a seismic wave carries, expressed in some reasonable coordinate system. If we choose to use geographic coordinates, we could use North-South (N), East-West (E), and Depth (D). We would then express the entire response as a 3x3xNt cube:

$$e(t) = \begin{bmatrix} e_{EE}(t) & e_{EN}(t) & e_{ED}(t) \\ e_{EN}(t) & e_{NN}(t) & e_{ND}(t) \\ e_{ED}(t) & e_{ND}(t) & e_{DD}(t) \end{bmatrix}. \quad (1)$$

However, the DDS has no coverage in the depth direction, so we are not able to estimate any elements of Equation 1 that contain a 'D' in their name. In fact, we can only solve the reduced problem of finding the 3 independent components of

$$e = \begin{bmatrix} e_{EE} & e_{EN} \\ e_{EN} & e_{NN} \end{bmatrix} \quad (2)$$

So, our goal is to build a "machine" that outputs 3 traces, whose sample points represent $e_{NN}(t)$, $e_{EN}(t)$, and $e_{EE}(t)$. This would then be a 3x3xNt cube, of the form

$$e(t) = \begin{bmatrix} e_{EE}(t) & e_{EN}(t) \\ e_{EN}(t) & e_{NN}(t) \end{bmatrix} \quad (3)$$

Let us specify the field system precisely, by letting the UTM grid N axis be the vertical axis and the grid E axis be the horizontal axis in a 2D Cartesian grid. In this system the northing and easting unit vectors are

$$\hat{t}_N = \begin{bmatrix} 0 \\ 1 \end{bmatrix} \text{ and } \hat{t}_E = \begin{bmatrix} 1 \\ 0 \end{bmatrix}. \quad (4)$$

Each of the fibre line segments have directional unit vectors as well, and there are eight of these:

$$\hat{t}_1 = \begin{bmatrix} t_1^1 \\ t_1^2 \end{bmatrix},\ \hat{t}_2 = \begin{bmatrix} t_2^1 \\ t_2^2 \end{bmatrix}, \ldots, \hat{t}_8 = \begin{bmatrix} t_8^1 \\ t_8^2 \end{bmatrix}. \quad (5)$$

Determining all of these unit vectors from GPS survey information for the DDS, we can then form a linear system relating the actual strain-rate (or strain if we integrate with respect to time) arriving at the sensor at a particular instant, in the field system, to those being sensed in the eight fibre loop directions:

$$\begin{bmatrix} e_1 \\ \vdots \\ e_8 \end{bmatrix} = L \begin{bmatrix} e_{EE} \\ e_{EN} \\ e_{NN} \end{bmatrix}, \quad (6)$$

where e_1 through e_8 single traces from each side of each square of the DDS after processing to approximate a point-receiver,

$$L = \begin{bmatrix} \lambda_{EE}^1 & 2\lambda_{EN}^1 & \lambda_{NN}^1 \\ \vdots & \vdots & \vdots \\ \lambda_{EE}^8 & 2\lambda_{EN}^8 & \lambda_{NN}^8 \end{bmatrix}, \quad (7)$$

and

$$\lambda_{AB}^{i} = (\hat{t}_i \cdot \hat{t}_A)(\hat{t}_i \cdot \hat{t}_B), \quad (8)$$

with *A*, *B* ranging over *E*, *N*. Given variable directional coverage from the DDS, this is an overdetermined system which can be solved for the three independent components of strain:

$$\begin{bmatrix} e_{EE} \\ e_{EN} \\ e_{NN} \end{bmatrix} = (L^T L + \alpha I)^{-1} L^T \begin{bmatrix} e_1 \\ \vdots \\ e_8 \end{bmatrix}. \quad (9)$$

Results

Examination of source gathers with receiver apertures greater than 10 m from the CamI.FRS show that data for this study will be dominated by aliased dispersive ground-roll. It is clear we will not be able to easily estimate time-series of strain-rate or strain tensors for reflections recorded on the DDS unless we acquire source gathers with larger source-receiver offsets. Given this, we proceed using the first identifiable peak corresponding to ground-roll arrivals for proof of concept.

DDS fiber traces with no contributions from the rounded square corners or adjacent sides of the DDS were extracted to form trace gathers for each side of each square. The gathers were then linear-moveout corrected to align the ground-roll and stacked to approximate a point receiver. Equivalent strain-rate traces were calculated for each side of the DDS from the surface geophones by rotating horizontal components to in-line with DDS side, subtracting two traces, and locating the resulting trace halfway along the DDS side (see Hall et al., (2020) for details).

Our expectation for VP1, VP2 and VP3 is that e_{NN} should have the most energy and e_{EN} should have the least. In contrast VP4 should have the most energy on e_{EE} and the least on e_{EN}. Figure 2 shows strain-rate tensors $e_{EE}(t)$, $e_{EN}(t)$ and $e_{NN}(t)$ estimated using Equation 9 for a time window defined by horizon picks TREF1 and TREF2 +/- 25 samples. Gathers are individually scaled for display. The straight and helical fibre tensors plot practically on top of each other, and the geophone results are very similar, although with higher relative amplitudes for VP2 ($e_{EE}(t)$ and $e_{EN}(t)$) and VP4 ($e_{EN}(t)$). The results match our expectations prior to doing the calculations (Figure 2).

Discussion and Future work

The prototype multicomponent DAS sensor was designed with a 5-10m gauge length in mind and given this limitation we view these results as being positive, and strongly indicative of the possibilities of the approach. However, the large size of the loop required in such a design, and the pre-processing it makes necessary (in order to create the dataset which would have been measured if the same parts of the seismic wave-front arrived at all points on the loop simultaneously), has led to fairly serious uncertainties. We regard the design and burial of a next generation of sensor loop, in which the lengths are on the order of 2m, and interrogation of this sensor with gauge lengths on the order of 1m, to be a critical next step.

Our present analysis is also suggestive that any further pre-processing for validation purposes would also be made significantly simpler if there were regions of the data dominated by body wave energy; more distant vibe points are indicated. Both the use of smaller gauge lengths and more distant vibe points will tend to exacerbate SNR issues in the data. For validation purposes this can probably be overcome with increased source effort.

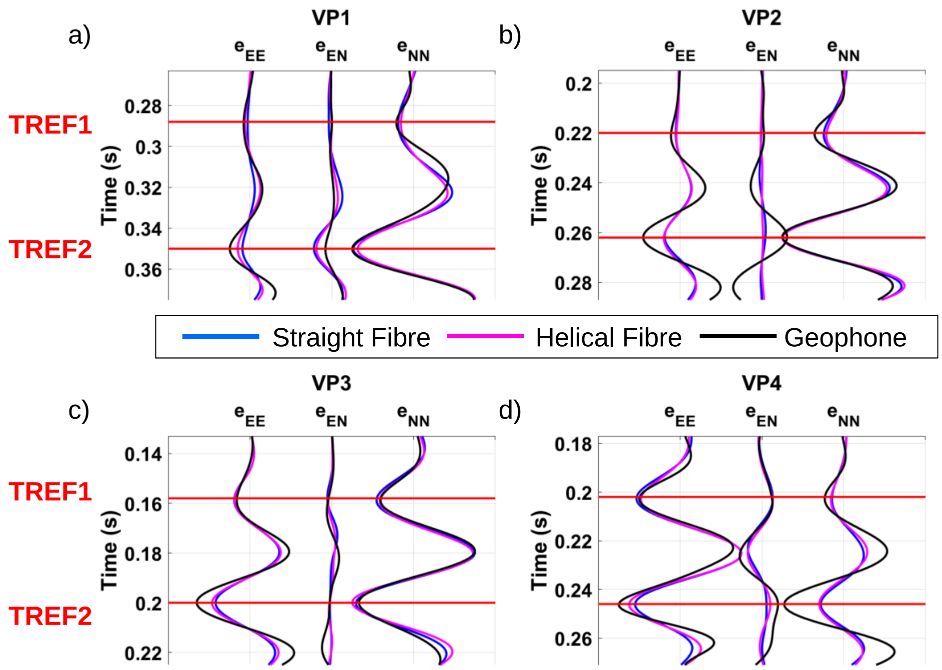

Figure 2. Time-series strain-rate tensors estimated for the first identifiable ground-roll peak for VP1 (a), VP2 (b), VP3 (c), and VP4 (d). Strain-rate traces were aligned on the troughs preceding (TREF1) and following (TREF2) the first identifiable ground-roll peak before applying Equation 9.

Acknowledgements

The sponsors of CREWES are gratefully thanked for continued support. This work was funded by CREWES industrial sponsors, NSERC (Natural Science and Engineering Research Council of Canada) through the grants CRDPJ 461179-13 and CRDPJ 543578-19, and in part by an NSERC-DG. We would also like to thank Halliburton for the field acquisition, Schlumberger for the use of donated Vista software, and all CREWES sponsors and CaMI.FRS JPI subscribers for their continued support.

References

Hall, K. W., Lawton, D. C., Daley, T., Freifeld, B., Marchesini, P., and Cook, P., 2018, Effect of source effort and source distance on optical fibre data at CaMI.FRS, Newell County, Alberta: 88th Annual International Meeting, SEG, Expanded Abstracts.

Hall, K. W., Innanen, K. A. H., and Lawton, D. C., 2020, Comparison of multi-component seismic data to fibre-optic (DAS) data: 90th Annual International Meeting, SEG, Expanded Abstracts.

Innanen, K. A. H., Lawton, D. C., Hall, K. W., Bertram, K. L., Bertram, M. B., and Bland, H. C., 2019, Design and deployment of a prototype multicomponent Distributed Acoustic Sensing loop array: 89th Annual International Meeting, SEG, Expanded Abstracts.